414 KSME Journal, Vol. 8, No. 4, pp. 414~421, 1994

Flow Visualization of Grid Generated Turbulence Under Stable Thermal Stratification

Kyunghwan Yoon*

(*Received March 5, 1994*)

We demonstrated the evolution of grid turbulence under the action of a stable, linear, temperature gradient with smoke-wire method. The experiment was carried out in a large, open circuit, low speed wind tunnel 0.91 × 0.91 m^2 and 9.14 m in length specially designed for the study of stratified turbulence. The smoke was generated by heating a thin nichrome wire coated with heavy-weight oil and the facility to take the pictures was controlled by a computer for the consistant shots. The temperature gradient, formed at the entrance to the plenum chamber of the tunnel by means of an array of 72 horizontal, differentially heated elements was 0℃/m for the unstratified case and 55℃/m for the stratified case where a Brunt-Väisälä frequency N was 1.3 s^{-1}. The grid mesh size M was 2.54 cm and the mean velocity U was fixed at 2.8 m/s for both cases. Thus the mesh Froude number $Fr_M = U/(NM)$ was ∞ and 84.8 for the unstratified and stratified case respectively. We show that there are distinct differences in the evolution of the flow for the stable case, especially, the vertical motion decays much more rapidly than for the neutral (unstratified) case. No evidence of internal wave motion is found from the flow visualization pictures.

Key Words: Turbulence, Flow Visualization, Stratified Flow, Smoke-Wire Method, Wind Tunnel

1. Introduction

The effect of a vertically decreasing density gradient on turbulent flow in a gravitational field is of singular importance in the atmosphere and is of considerable importance in industrial flows. In the atmosphere the density decrease (affected by a "temperature inversion," ie., an increase in temperature with height) occurs on most evenings over land and frequently during the day over regions of unusual topography or proximity to the sea, for example Mexico City or Los Angeles. The inversion suppresses the turbulence and can reduce the effective diffusivity of the atmosphere by as much as 10^6 (the ratio of the turbulent diffusivity to molecular diffusivity). Clearly accurate prediction and control of pollution concentrations depends largely on an understanding of the underlying turbulence dynamics for these conditions. Even in pipe flow, particularly in reactor design, thermal stratification can lead to boiling resulting in bowed and cracked pipes. Other examples abound. Much of the work (up to the early 1970's) concerning our experimental and theoretical understanding of stratified fluids is summarized well in Turner(1973). A useful review of more recent work is provided by Hopfinger(1987).

A proper understanding of the problem even for the simplest case, vis. an initially isotropic turbulent field evolving in a region in which the (potential) temperature is increasing linearly with height is still wanting. The difficulty is most simply understood by recognizing there is a complex interaction of two dynamic scales, one due to the mechanical turbulence, the other resulting from the thermal stratification.

In this paper we consider the evolution of grid generated turbulence under the influence of a

* Department of Mechanical Engineering, Dankook University, Seoul, Korea

linear stable density gradient using a smoke-wire method as a flow visualization tool. This is the simplest situation in which to study the effects of stratification on turbulence ; there is no shear and the turbulence is initially (before the buoyancy effects begin to play a role) close to isotropic. Assuming homogeneity in the vertical (y-z) plane the equations for the averaged turbulence kinetic energy $k=\frac{1}{2}(\overline{u^2}+\overline{v^2}+\overline{w^2})$ and its components $\frac{1}{2}\overline{u^2}$, $\frac{1}{2}\overline{v^2}$ and $\frac{1}{2}\overline{w^2}$, the kinematic vertical heat flux $\overline{\theta w}$ and the mean squared temperature variance, $\overline{\theta^2}$, are (eg. Lumley and Panofsky 1964).

$$U\frac{\partial k}{\partial x}=-\frac{g}{T_0}\overline{\theta w}-\varepsilon \tag{1}$$

$$U\frac{\partial(1/2\,\overline{u^2})}{\partial x}=-\frac{1}{\rho_0}\overline{p\frac{\partial u}{\partial x}}-\nu\overline{\frac{\partial u}{\partial x_j}\frac{\partial u}{\partial x_j}} \tag{1a}$$

$$U\frac{\partial(1/2\,\overline{v^2})}{\partial x}=-\frac{1}{\rho_0}\overline{p\frac{\partial v}{\partial x}}-\nu\overline{\frac{\partial v}{\partial x_j}\frac{\partial v}{\partial x_j}} \tag{1b}$$

$$U\frac{\partial(1/2\,\overline{w^2})}{\partial x}=-\frac{1}{\rho_0}\overline{p\frac{\partial w}{\partial x}}-\nu\overline{\frac{\partial w}{\partial x_j}\frac{\partial w}{\partial x_j}}+\frac{g}{T_0}\overline{\theta w} \tag{1c}$$

$$U\frac{\partial\overline{\theta w}}{\partial x}=-\overline{w^2}\beta+\frac{g}{T_0}\overline{\theta^2}-\frac{1}{\rho_0}\overline{\theta\frac{\partial p}{\partial z}} \tag{2}$$

$$U\frac{\partial(1/2\,\overline{\theta^2})}{\partial x}=-\overline{\theta w}\beta-\varepsilon_\theta \tag{3}$$

Here U is the mean velocity (in the x direction) which is constant throughout (excepting in the boundary layers of the tunnel which are very small compared to the free stream region and are not of interest in this study) ; g is the acceleration due to gravity (acting in the z direction). T_0 and ρ_0 are the reference temperature and density respectively ; u, v and w are the longitudinal, transverse and vertical fluctuating velocity components, θ is the fluctuating temperature, $\beta\equiv dT/dz$ is the vertical temperature gradient, p is the fluctuating pressure, ε is the dissipation rate of the velocity fluctuations ($\equiv\nu\overline{\frac{\partial u_i}{\partial x_j}\frac{\partial u_i}{\partial x_j}}$ where ν is the kinematic viscosity) and ε_θ is the destruction rate of temperature variance by molecular smearing ($\equiv\alpha\overline{\frac{\partial\theta}{\partial x_j}\frac{\partial\theta}{\partial x_j}}$ where α is the thermal diffusivity). The overbars represent averaging. A sketch of the tunnel with the co-ordinate system is given in section 2. It should be noted that (as a consequence of Eq. (2)) if the turbulence is homogeneous in the z direction and β is initially constant then β will remain constant and is independent of x. This was first pointed out by Corrsin(1952).

The physical significance of the terms in the above equations is described in the standard texts (Lumley and Panofsky 1964, Monin and Yaglom 1971). The gravitational terms (first term on the right hand side of 1 and second term on the right hand side of 2) have a profound effect on the development of the velocity and thermal fields. The strength of the stable stratification is usually expressed in the form of the Brunt-Väisälä frequency $N\equiv[(-g/\rho_0)\partial\bar{\rho}/\partial z]^{1/2}=[(g/T_0)\beta]^{1/2}$ $\sec^{-1}$. Note that for the passive case $N\sim 0$. While the mesh size M determines the initial scale of the velocity fluctuations, their subsequent evolution is determined by the complex interaction of the turbulence dissipation and the stable stratification, the latter, we will show, assuming an ever increasing role as the flow evolves (close to the grid the flow behaves passively).

Grid generated stratified tunnel experiments that are related to the present work have been done by Lienhard(1988) and Lienhard and Van Atta(1990), Britter et al.(1983), Dickey and Mellor(1980), Itsweire et al.(1986), Montgomery(1974) and Stillinger et al.(1983). For an overview of subject from a geophysical perspective the reader is referred to volume 92, no. 5 (1987) of the Journal of Geophysical Research which devoted to papers from the IUTAM conference on mixing in stratified flows(Imberger, 1987).

The broad objective of the present paper is, then, to study the effect of a stable density gradient on isotropic turbulence qualitatively by using a smoke-wire method. This kind of flow visualization has not done so far for the wind tunnel experiment. The work, in many respects, follows from our earlier experiments on the evolution of heat flux and temperature variance under the action of a passive linear temperature gradient (Sirivat and Warhaft 1983) and active linear temperature gradient case (Yoon, 1989; Yoon and Warhaft, 1989).

2. Experimental Apparatus and Instrumentation

2.1 The wind tunnel and heater

The experiment was carried out in a new large, low speed, low background turbulence wind tunnel specially designed for stratified flow studies. A sketch of the tunnel is shown in Fig. 1. Apart from the heater element section the tunnel is of standard open circuit suction design. The test section was 91×91 cm square and 9.1 m long. The large cross section area allowed for a large isotropic core to persist to the end of the tunnel in spite of the development of the boundary layers. The mesh length M of the square bar biplanar brass grid was 2.54 cm, giving a longitudinal tunnel extent of 360 M and vertical and horizontal dimensions of 36 M. The solidity of the grid (ratio of closed to projected area) was 0.34. One of side walls was slightly divergent to ensure a constant centerline mean speed with the development of the boundary layer. The test section was wooden (1.9 cm ply) and covered with 5.08 cm fiber glass insulating sheets. Pictures were taken through 4 side windows and its position was 70, 110, 150, 190 M apart from the grid position. For our experiment the mean test section velocity was fixed at 2.8 m/s which is the lowest stable speed with this tunnel to find the strongest effect of buoyancy. The hot air was exhausted through a window to the outside of laboratory to avoid unwanted feedback.

The design principle of the heater, plenum and contraction was to produce a linear temperature gradient in as low background turbulent flow as possible so that by the time the flow reached the grid there would be a linear temperature gradient in laminar flow. Thus the temperature fluctuations in the test section would be due solely to the action of the grid generated turbulence against the temperature gradient. This is the same as the "toaster" approach used by Sirivat and Warhaft (1983) although here, because of the larger gradient required, a different heater design was necessary.

The heater, placed at the entrance to the plenum, consisted of 72 horizontal 2.74 m long, equally spaced elements. They were nichrome ribbons inserted through 9.53 mm outside diameter porcelain tubes. The ribbons were 0.127 mm

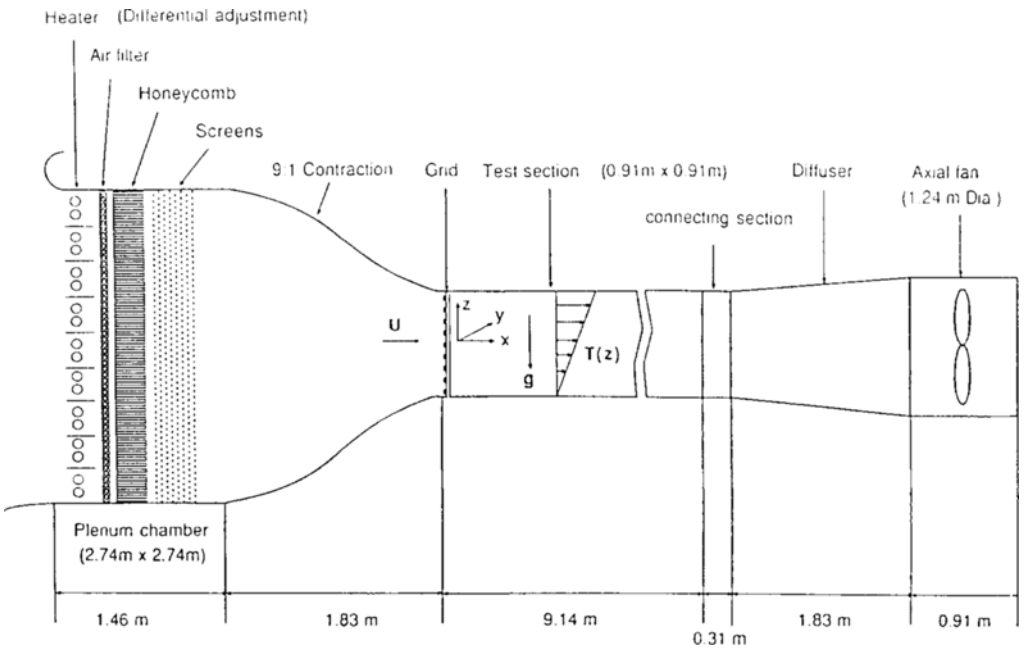

Fig. 1 Sketch of the stratified wind tunnel. Note, there are 72 heater elements (only 18 are shown in the sketch)

thick and 6.35 mm wide for the top 32 elements (where more heat was required) and 0.1 mm × 4.76 mm for the bottom 40 elements. Their resistances were 1.37 Ω/m and 2.26 Ω/m respectively (at room temperature). Black aluminum plates of cross section area 20.3 cm × 1.6 mm were placed horizontally between every second element to reduce radiation losses (see Fig. 1 Note that only 18 of the 70 elements are shown in the sketch). The heater elements were differentially controlled to produce the linear temperature gradient. A trial and error "tuning" approach was used to obtain the linear profile. The top 32 rods could be heated to 5 kw maximum and the bottom 40 rods to 2.5 kw. The total power required for the temperature gradient used (55℃/m) was approximately 60 kw. Three thin vertical aluminum rods were equally spaced and fastened to the heating rods in order to stop sagging of the elements. Further design details are in Yoon(1989).

The heated air produced by the elements first passed through an air filter which removed all particles down to 1 μm. To reduce swirl and lateral mean velocity fluctuations the air then passed through a low heat conductivity (polycarbonate) set of honeycombs of 1.905 cm cell diameter and 15.24 cm length. This was followed by eight fine wire screens in order to dampen the turbulence. The solidity of the screens was 0.373, their wire diameter was 0.165 mm and their mesh size was 0.0794 cm. They were placed 7.6 cm apart (ie. approximately 100 screen mesh lengths) so that ample decay occurred before the next screen (Weighart, 1953). After the screens the flow was accelerated through the 9 : 1 asymmetric contraction. Both the plenum chamber and the contraction section were insulated with fiber glass sheets to avoid heat loss.

2.2 The apparatus and flow visualization system

Mean velocity and temperature were measured using standard pitot tubes and Chromel-Constantan thermocouples. Also the longitudinal velocity was measured with U-type hot wire in conjunction with Dantec 55 M01 constant temperature bridges. The length to diameter ratio of the 3.05 μm tungsten wires was 200. The data was then analyzed on a Micro Vax II computer. A standard statistical program (STAT version 2.0, K. Yoon & S. Veeravalli) was used in order to calculate the various moments, spectra and pdf's (see details in Yoon 1989).

The set-up for the flow visualization is shown in Fig. 2. The diameter of 0.005" nichrome wire, which was placed 30 Mesh length up-steam from the window, was used and it was rolled on the pulley driven by a step motor. Heavy motor oil (15 W-40 Kendall or Nitro 70-Turbo) was coated througth the roller which is half-immersed in the oil vessel. The reason why we selected heavy weight oil was it does not melt at high temperature in our experimental condition. Various paraffins have been tested but they did not give enough quality what we wanted. Most of cases for using paraffins we could not get consistant shots because of the uneven coating and rack of intensity.

A normal 35 mm camera (Cannon T50) and two flashes were used. One of flash was trigerred by the other flash through a light trigger swith pack. To give a better constrast the opposite side wall to the picture-taking window was covered black hard-board and a narrow mirror was positioned at the top middle section. Fast color films of ASA 400 and 1000 were used f/stop was 1.8 and 2.8 for normal angle 50 mm lens. Wide

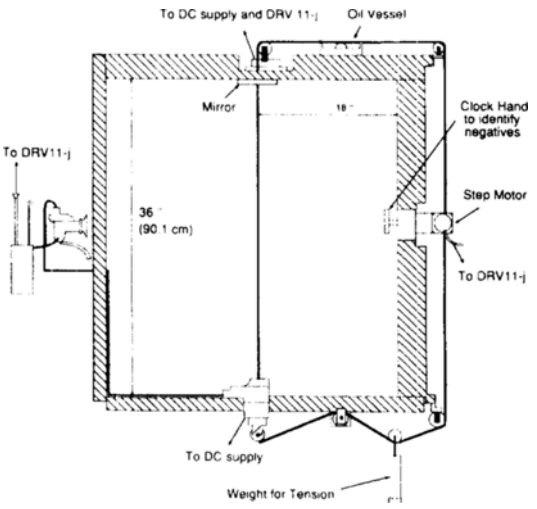

Fig. 2 Experimental set-up for the flow visualization

angle lens were used to verify the homogeneity of the field.

The top and bottom plugs were connected to DC power supply (5 Amp. 60 Volts. max.). This DC is important becuase we found the vibrations of the smoke-wire with AC power supply in the early stage of this project.

Winding of the nichrome wire, starting and disconnecting time of heating eletricity and opening time of camera sutter were controlled by micro Vax II computer through DRV 11-J.

2.3 Wind tunnel performance

The turbulence intensity $\sqrt{\overline{u^2}}/U$ of the flow just before the grid was 0.25% and the background temperature noise (heaters off) was approximatley 0.025℃ rms. The centerline mean velocity (after adjusting the side wall) varied by $\pm 0.5\%$ over the tunnel length. At the furthest downstream measurement station (340 M) the boundary layer was 6 M, still providing a large core flow since the tunnel area is 36×36 M.

The mean temperature profiles along the test section for the stratified case is very good. The mean temperature (for a fixed z) varies by less than 5% along the tunnel and the gradient in the z direction is remarkably stable and constant over at least 12 M in the z direction (for the worst case). The variation of the velocity variances across the core of the flow was comparable(Yoon 1989).

Figures 3 shows the picture of smoke lines for the stratified case without grid, it can be seen a laminar flow pattern without any wave motion. This picture was taken as a check for the performance of the tunnel and the smoke-wire method itself. We show only one picture for this case because the pictures taken at the other locations were identical.

3. The Results

As explained in the introduction, the emphasis of this work will be on the evolution of vertical motion of the flow under the action of stable condition. The stably stratified case will be compared with the neutral case. The detailed flow parameters and quantities for the neutral and stratified case investigated can be found in Yoon and Warhaft(1990), which will be compared with present flow visualization pictures as a guildline.

3.1 Vertical motion of the flow related to the vertical velocity variance

Figure 4 shows the evolution of the vertical variances, $\overline{w^2}/U^2$, for the unstratified and stratified cases, plotted as a function of x/M. The straight line is the best fit for a number of passive experiments from Yoon and Warhaft(1990). As would be expected the effects of the negative buoyancy are very much pronounced. The data show three stages : initially the variance decays at approximately the same rate as for the passive case, it then decays more rapidly as the buoyancy effects become more pronounced and finally ($x/M \sim 200$) the variance begins to decay at a much

Fig. 3 The smoke line picture without grid for $\beta =$ 55℃/m, U=2.8 m/s (The yellow stick is a clock hand to identify the condition for each shot)

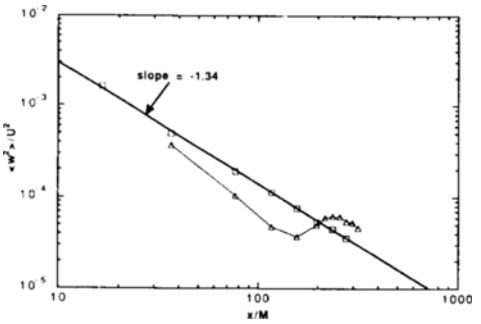

Fig. 4 The vertical velocity variance, $\overline{w^2}/U^2$ as a function of x/M. The straight line is the best fit for a number of passive cases. △, $Fr_M = 84.8$ (stratified) ; □, $Fr_M = \infty$ (unstratified)

slower rate (or the vertical component even increases) than for the passive flow. Notice for the stratified case, far downstream w^2 actually increases indicating that vertical kinetic energy is being supplied to the flow, ie. the kinetic energy earlier extracted from the flow by the negative buoyancy is being fed back. Finally, for this case too the variance decreases again as shown in Fig. 4. A similar oscillatory effect where kinetic and potential energy are exchanged has been shown in the numerical simulations of Riley et al.(1981).

Figures 5(a) and (b) show the picture of smoke lines for the unstratified and stratified cases respectly taken at 70 M from the grid. There is strong turbulent motion in both cases, so we can not identify the effect of strong stratification. Note that all the vortices are well distributed isotropically. Figures 6(a) and(b) show the pictures for the unstratified and stratified cases respectly taken at 110 M from the grid. There is still strong turbulent motion for the unstratified case compared with less vortices shown for the stratified case. Figures 7(a) and (b) show the picture of smoke streaks for the unstratified and stratified cases respectly taken at 150 M from the grid. The biggest difference can be found between two cases. For the stratified case the vertical motion was almost suppressed by the effect of buoyancy. However, for the neutral case well distributed three dimensional structure can be found. Figures 8(a) and (b) show the pictures taken at 190 M from the grid. Turbulent motion has been decayed in both cases, however, the small packets of vortical motion still remains. The interesting thing is the vertical movement of each streak lines are comparable in both cases as shown earlier in Fig. 4 and Yoon and Warhaft (1990) from the data of vertical velocity variance.

3.2 The relation to the heat flux

As shown in our earlier work (Yoon and Warhaft 1990) the ability of stable stratification to inhibit turbulent mixing is most clearly mainifest in the evolution of the vertical turbulent heat flux, $\rho_0 C_p \overline{w\theta}$. From Eq. (1c) we can see that this vertical heat flux term appears only in the evolution of the vertical kinetic energy. Although here, from the pictures taken, we cannot calculate

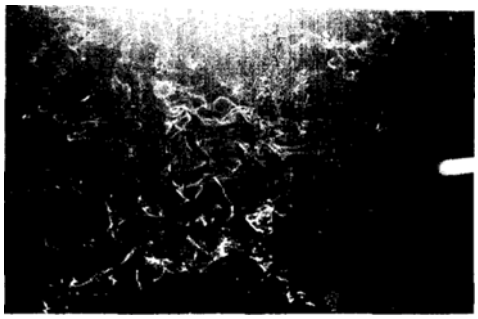

(a) unstratified

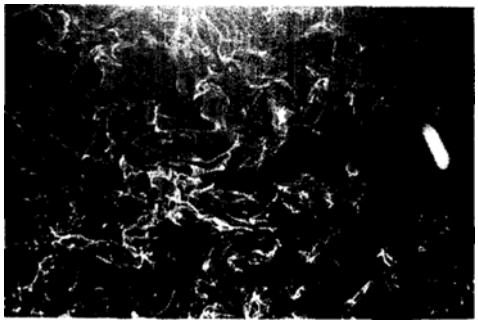

(b) stratified ($Fr_M = 84.8$)

Fig. 5 The smoke line pictures with mesh length of 2.54cm grid at x/M=70

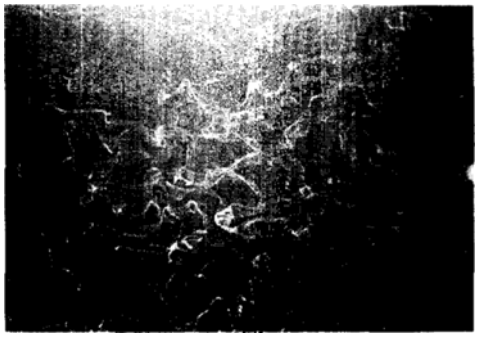

(a) unstratified

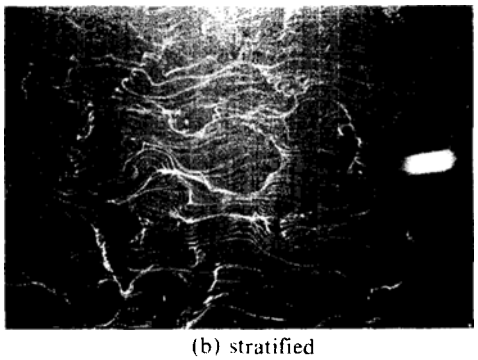

(b) stratified

Fig. 6 Same as Fig. 5 but at x/M=110

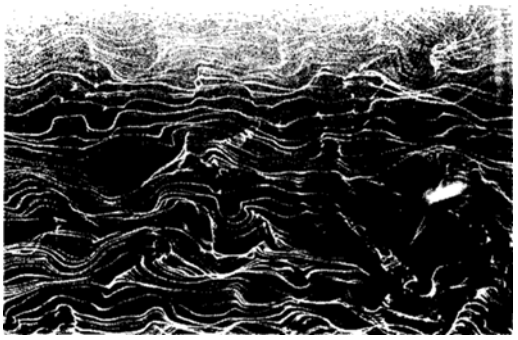

(a) unstratified

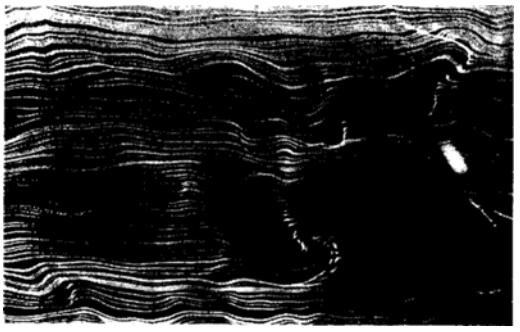

(b) stratified

Fig. 7 Same as Fig. 5 but at x/M = 150

(a) unstratified

(b) stratified

Fig. 8 Same as Fig. 5 but at x/M = 190

the quantitative mixing rate the turbulent mixing can be found with a vetical motion. Also the trace of the each streak lines of smoke revealed that the flow is not a distinct gravitaional wave motion within the range of our observation even after the first collapse of the turbulent heat flux which was observed in salt-water experiment.

4. Conclusions

The effects of stable stratification on the evolution of grid generated turbulence are profound, producing a complex interaction between the fluctuating kinetic energy and potential energy fields that can completely suppress turbulent transport and even result in regions of counter gradient heat flux. In this study, using a new large low speed wind tunnel, the mesh Froude number $Fr_M = U/(NM)$ was fixed (by means of changing the temperature gradient)∞(unstratified) and 84.8 ($dT/dz = 55$℃/m).

A contradictory finding about the presence of gravity wave after the first collapse of the turbulent heat flux has been observed to compare the present result with the results of previous flow visualization using salt-water tank.

Neither Lienhard and Van Atta (1990) or Riley et al. (1981) observe the presence of internal gravity waves and our present results from flow visualization and the previous one point measurement (Yoon and Warhaft, 1990) are in accord with this finding. If gravity waves are present more subtle detection methods (such as multipoint measurements) will be needed in the future to reveal them.

In a technical point of view, developing a more refined smoke-wire method is recommended for controling the number of streak lines per unit length and the intensity of smoke for different temperature.

References

Britter, R. E., Hunt, J. C. R., Marsh, G. L. and Snyder, W. H., 1983, "The Effect of Stable Stratification on Turbulent Diffusion and the Decay of Grid Turbulence," *J. Fluid Mech.*, Vol. 127, pp.

27~44.

Corrsin, S., 1952, "Heat Transfer in Isotropic Turbulence," *J. Appl. Phys.*, Vol. 23, pp. 113~118.

Dickey, T. D. and Mellor, G. L., 1980, "Decaying Turbulence in Neutral and Stratified Fluids," *J. Fluid Mech.*, Vol. 99, part 1, pp. 13~31.

Hopfinger, E. J., 1987, "Turbulence in Stratified Fluids: A Review," *J. Geophys. Res.*, Vol. 92, No. C5, pp. 5287~5303.

Itsweire, E. C., Helland, K. N. and Van Atta, C. W., 1986, "The Evolution of Grid-Generated Turbulence in a Stably Stratified Fluid," *J. Fluid Mech.*, Vol. 162, pp. 299~388.

Imberger, J., 1987, "Introduction to Papers from the IUTAM Symposium on Mixing in Stratified Fluids," *J. Geophys. Res.*, Vol. 92, No. C5, p. 5229.

Lienhard, J. H., 1988, "The Decay of Turbulence in Thermally Stratified Flow," Ph D. Dissertation, University of California at San Diego.

Lienhard, J. H. and Van Atta, C. W., 1990, "The Decay of Turbulence in Thermally Stratified Flow," *J. Fluid Mech.*, Vol. 210, pp. 57~112.

Lumley, J. L. and Panofsky, H. A., 1964, *The structure of atmospheric turbulence*, Interscience, New York.

Montgomery, R. D., 1974, "An Experimental Study of Grid Turbulence in a Thermally-Stratified Flow," Ph. D. Dissertation, University of Michigan.

Monin, A. S. and Yaglom, A. M., 1975, *Statistical Fluid Mechanics*, Vol. I & II, MIT Press, Cambridge.

Riley, J. J., Metcalfe, R. W. and Weissmann, M. A., 1981, "Direct Numerical Simulation of Homogeneous Turbulence in density-Stratified Fluids," In *Nonlinear properties of internal waves*, ed. B. J. West. AIP Conference Proc., Vol. 76, pp. 79~112.

Sirivat, A. and Warhaft, Z., 1983, "The Effect of a Passive Cross-Stream Temperature Gradient on the Evolution of Temperature Variance and Heat Flux in Grid Turbulence," *J. Fluid Mech.*, Vol. 128, pp. 323~346.

Stillinger, D. C., Helland, M. J. and Van Atta, C. W., 1983, "Experiments on the Transition of Homogeneous Turbulence to Internal Waves in a Stratified Fluid," *J. Fluid Mech.*, Vol. 131, pp. 501~528.

Turner, J. S., 1973, *Buoyancy Effects in Fluids*, Cambridge University Press, Cambridge.

Weighart, K. E. G., 1953, "On the Resistance of Screens," *Aero. Quart.*, Vol. 4, p. 186.

Yoon, K. 1989, "The Effect of Stable Stratification on Decaying Grid-Generated Turbulence," Ph. D. Dissertation, Cornell University.

Yoon, K. and Warhaft, Z., 1990, "The Evolution of Grid Generated Turbulence under Conditions of Stable Thermal Stratification," J. F. M., Vol. 215, pp. 601~638.